Mechanism for the Retardation of the Acid Dissolution Rate of Hydroxyapatite by Strontium

MAHENDRA G. DEDHIYA, FUDAH YOUNG, and WILLIAM I. HIGUCHI

College of Pharmacy, University of Michigan, Ann Arbor, Michigan 48104, USA

Dissolution rates and apparent solubilities for synthetic hydroxyapatite in acetate buffers containing phosphate and strontium ions in the range of 10^{-3} to 10^{-2} M were determined under various pH and buffer conditions. Critical examination of the role of strontium with a physical model suggests that a calcium-strontium apatite surface complex may govern the driving force of the dissolution reaction.

In recent years there has been an increasing awareness of the possible influence of trace elements on the inhibition of dental caries.[1] The available evidence has been qualitative and sometimes controversial.[2] Thus, it would be of considerable interest from a physicochemical standpoint to determine the roles played by ions other than the principal ions of hydroxyapatite in inhibiting the acid attack of the enamel mineral.

One of the trace elements of interest to investigators in caries research is strontium.[3] There have been clinical studies and some in vitro studies[4] of the possible relationship of strontium to caries. However, the possible mechanistic role of this element in the caries process has not been determined.

In this report, a critical investigation of the influence of strontium on hydroxyapatite dissolution rates in acidic media is presented; the physical model approach was used as the principal technique for data evaluation. Systematic analysis points strongly to the interpretation that the dissolution rate of hydroxyapatite in aqueous media containing strontium may be governed by a surface apatitic complex with the composition $Ca_6Sr_4(PO_4)_6(OH)_2$, and with energy comparable to the parent surface counterpart, $Ca_{10}(PO_4)_6(OH)_2$.

Received for publication November 30, 1972.

Materials and Methods

CALCIUM-STRONTIUM APATITE SURFACE COMPLEX MODEL.—In the physical model it is assumed that when hydroxyapatite crystals are exposed to acid buffers containing sufficiently high concentrations of strontium ions, a thin layer of a calcium-strontium apatite complex, $Ca_{10-n}Sr_n(PO_4)_6(OH)_2$, is formed rapidly around the crystal surfaces by the following reaction:

$$Ca_{10}(PO_4)_6(OH)_2 + nSr^{2+} \rightarrow Ca_{10-n}Sr_n(PO_4)_6(OH)_2 + nCa^{2+}, \quad (1)$$

where n, an integer in the range of $0 \leqslant n \leqslant 10$, is the number of strontium ions participating in the substitution reaction at the apatite crystal surface. It also is assumed that this complex governs the ambient solution conditions at the crystal-solvent interface.

The transport of the various molecular and ionic species is determined by the strontium substitution reaction (equation 1) and the reaction taking place in the acid buffer solvent:

$$Ca_{10-n}Sr_n(PO_4)_6(OH)_2 + 8H^+ \rightarrow (10-n)Ca^{2+} + nSr^{2+} + 6HPO_4^{2-} + 2H_2O. \quad (2)$$

The basic model for these processes is shown in Figure 1. During dissolution, the acid species diffuse toward the crystal-liquid interface ($x = 0$), and calcium and phosphate ions diffuse toward the bulk in the liquid diffusion layer of thickness h ($x = h$). Thus, this model is based on the assumption that the dissolution of hydroxyapatite crystals in an acid buffer that contains a constant level of strontium ions is controlled by the activity product[a] of the calcium-strontium

[a] This activity product could be defined better as that which the calcium-strontium apatite complex is able to yield under the dynamic reaction conditions.

apatite complex and the diffusion rates of various species involved.

The appropriate equations for this model are based on methods described in earlier studies[5,6] of enamel dissolution in acid media. For a one-dimensional problem (Fig 1), the following steady-state equations can be used to describe the simultaneous diffusion and chemical equilibria of the species in the diffusion layer per unit area:

$$D_{Ca^{2+}} \frac{d^2(Ca^{2+})}{dx^2} = 0 \quad (3)$$

$$D_{Sr^{2+}} \frac{d^2(Sr^{2+})}{dx^2} = 0 \quad (4)$$

$$D_{HPO_4^{2-}} \frac{d^2(HPO_4^{=})}{dx^2} - \theta_1 - \theta_2 = 0 \quad (5)$$

$$D_{H_2PO_4^-} \frac{d^2(H_2PO_4^-)}{dx^2} + \theta_1 + \theta_2 = 0 \quad (6)$$

$$D_{HB} \frac{d^2(HB)}{dx^2} - \theta_2 + \theta_3 = 0 \quad (7)$$

$$D_{B^-} \frac{d^2(B^-)}{dx^2} + \theta_2 - \theta_3 = 0 \quad (8)$$

$$D_{H^+} \frac{d^2(H^+)}{dx^2} - \theta_1 - \theta_3 = 0. \quad (9)$$

These expressions for diffusion take into account the mass balances of the chemical reactions of various species involved. The D's in the equations (3 to 9) are the respective diffusion coefficients,[b] where HB and B^- are the buffer acid molecule and its anion. In the present studies, they represent acetic acid and acetate ions, since acetate buffers were used. Quantities in the parentheses are terms expressing the concentrations of the respective species. The θ's are the rates of reaction per unit volume for the following reactions:

$$HPO_4^{=} + H^+ \rightarrow H_2PO_4^- \quad \theta_1$$

$$HPO_4^{=} + HB \rightarrow H_2PO_4^- + B^- \quad \theta_2$$

$$H^+ + B^- \rightarrow HB. \quad \theta_3$$

Along with the equations (3 to 9), the following equilibrium expressions apply at the crystal-liquid interface at any position in the diffusion layer, and in the bulk solvent, that is, at $x \geqslant o$

$$K_{2p} = \frac{(H^+)\ (HPO_4^{=})}{(H_2PO_4^-)} \quad (10)$$

$$K_{3p} = \frac{(H^+)\ (PO_4^{\equiv})}{(HPO_4^{=})} \quad (11)$$

$$K_{HB} = \frac{(H^+)\ (B^-)}{(HB)} \quad (12)$$

$$K_w = (H^+)\ (OH^-). \quad (13)$$

K_w is the ion product for water.

[b] The influences of the electric diffusion potential[7] also are neglected here. This should be a good assumption, especially since a swamping electrolite was presented in the experiments.

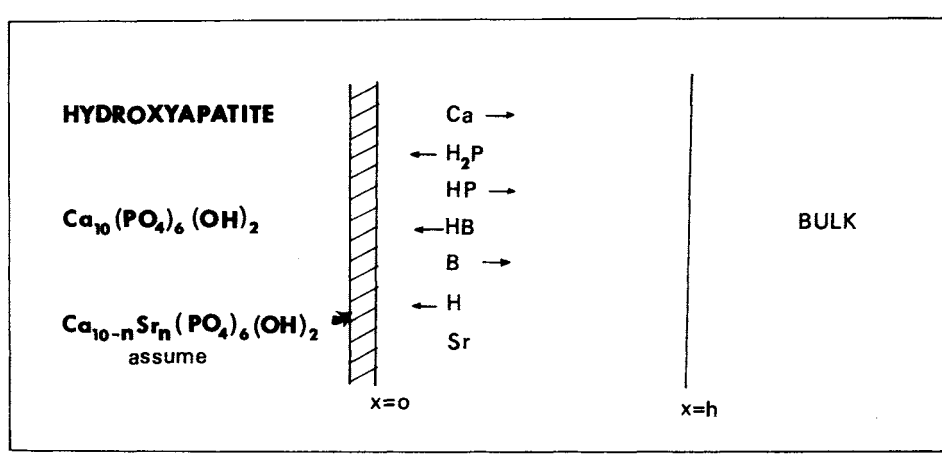

FIG 1.—Model for effect of strontium on hydroxyapatite dissolution in acid buffer solutions. A calcium-strontium apatite complex, $Ca_{10-n}Sr_n(PO_4)_6(OH)_2$, is assumed to form at apatite surface.

The activity product of the calcium-strontium apatite complex, K_{ap}, governs the equilibrium conditions at $x = o$, the crystal-solvent interface:

$$K_{ap} = (Ca^{2+})_o^{10-n} (Sr^{2+})_o^{n} (PO_4^{\equiv})_o^{6} (OH^-)_o^{2} \quad (14)$$

Eliminating all the θ's and assuming the conditions given by equations 1 and 2, equations 3 to 9 can be combined and integrated over the limits $x = o$ and $x = h$ to obtain a set of equations similar to those in earlier work,[5,6] except that the dissolution rate, J, is defined as the flux of total phosphate[c] in the liquid diffusion layer, namely,

$$J = -\left(D_{HPO_4^{\equiv}}\right)\frac{d(HPO_4^{\equiv})}{dx} - \left(D_{H_2PO_4^-}\right)\frac{d(H_2PO_4^-)}{dx} \quad (15)$$

Further integration of these equations over the limits $x = o$ and $x = h$ using equations 10 to 14 gave equations 16 and 17 (Fig 2). Equations 16 and 17 are the integral expressions derived from the proposed physical model.

DISSOLUTION RATE CALCULATIONS WITH THE MODEL.—The only unknown quantities in equations 16 and 17 are J, K_{ap}, $(H^+)_o$, and n. The other quantities may be estimated or determined from independent experiments.

[c] The concentrations of H_3PO_4 and $PO_4^{\equiv}$ in the acidic buffers studied are negligible compared with those of $H_2PO_4^-$ and $HPO_4^{\equiv}$.

$$\frac{4}{3}J = \frac{D_{H_2PO_4^-}}{h}\left\{(H_2PO_4^-)_h - \frac{J + \frac{D_{HPO_4^{\equiv}}}{h}(HPO_4^{\equiv})_h + \frac{D_{H_2PO_4^-}}{h}(H_2PO_4^-)_h}{\left[\frac{K_{2p}\frac{D_{HPO_4^{\equiv}}}{h}}{(H^+)_o} + \frac{D_{H_2PO_4^-}}{h}\right]}\right\} +$$

$$\frac{D_{HB}}{h}\left[(HB)_h - \frac{\frac{D_{B^-}}{h}(B^-)_h + \frac{D_{HB}}{h}(HB)_h}{\frac{D_{HB}}{h} + \frac{D_{B^-}}{h}\frac{K_{HB}}{(H^+)_o}}\right] + \frac{D_{H^+}}{h}\left[(H^+)_h - (H^+)_o\right] \quad (16)$$

$$K_{ap} = \frac{K_w^2 K_{3p}^6 K_{2p}^6}{(H^+)_o^{14}}\left[\frac{J}{0.6\frac{D_{Ca^{2+}}}{h}} + (Ca^{2+})_h\right]^{10-n}(Sr^{2+})_h^n \times$$

$$\left[\frac{J + \frac{D_{HPO_4^{\equiv}}}{h}(HPO_4^{\equiv})_h + \frac{D_{H_2PO_4^-}}{h}(H_2PO_4^-)_h}{\frac{\frac{D_{HPO_4^{\equiv}}}{h}K_{2p}}{(H^+)_o} + \frac{D_{H_2PO_4^-}}{h}}\right]^6 \quad (17)$$

FIG 2.—Equations 16 and 17.

J is the dissolution rate of hydroxyapatite expressed as moles of total phosphate transported per unit area, as defined by equation 15. K_{ap} is the activity product of the calcium-strontium apatite complex, $Ca_{10-n}Sr_n(PO_4)_6(OH)_2$, as defined by equation 14. $(H^+)_o$ is the concentration of hydrogen ions at the crystal-liquid interface ($x = o$), and n is the number of strontium ions participating in the formation of the calcium-strontium apatite complex. Mathematically, any two of these quantities can be calculated as a function of the other two by solving equations 16 and 17. When J is known, equations 16 and 17 can be solved numerically for $(H^+)_o$ and K_{ap} by proper digital computer programming for each preselected value of n. Values of all the parameters entering into equations 16 and 17 are listed in Table 1. J may be calculated from Je, the experimental dissolution rate, using the relation

$$J = \frac{1}{A} Je, \qquad (18)$$

where A is the total surface area of the hydroxyapatite. The factor $1/A$, may be obtained easily from similar experiments conducted in the absence of strontium acid data by use of the hydroxyapatite model[5,6] and a K_{hap} value of 1×10^{-132}.[5,6]

SOLUBILITY PRODUCT CALCULATIONS WITH THE MODEL.—When dissolution of hydroxyapatite in acid buffers containing known concentrations of strontium ions reaches an apparent equilibrium, the apparent solubility product, K_{ap}, can be determined by analyzing the calcium and total phosphate concentrations in the bulk. Such data can be obtained for each dissolution rate experiment. Equation 14, which is applicable to the bulk equilibrium conditions, then can be written

$$K_{ap} = (Ca)_h^{10-n} (Sr)_h^n (P)_h^6 (OH)_h^2, \qquad (19)$$

where the quantities in parentheses are concentrations in the bulk. $(Sr)_h$ is known and $(Ca)_h$ is analyzed. $(P)_h$ can be calculated by equation 20,

$$(P) = \frac{TP}{(1 + \frac{(H)}{K_{3p}} + \frac{(H)^2}{K_{2p}K_{3p}})}, \qquad (20)$$

where TP is the total phosphate analyzed in the bulk. If the pH of the bulk solution is known, $(OH)_h$ can be calculated by equation 13. Thus, from the determination of calcium, phosphate, and pH, the solubility product, K_{ap}, can be calculated as a function of n values according to equation 19.

DETERMINATION OF THE EXPERIMENTAL RATE OF DISSOLUTION AND THE APPARENT SOLUBILITY.—The dissolution rates and solubilities were determined with a pure and well-crystallized sample of powdered synthetic hydroxyapatite prepared according to procedures developed by the Tennessee Valley Authority Laboratory (TVA).[8] A similar sample was used in previous studies[5,6] in these laboratories. Reagent grade monosodium phosphate, strontium chloride, acetic acid, sodium acetate, and sodium chloride were used in preparing the acetate buffer solutions.

The experiments essentially involved observing buffered solutions. The dissolution of 100 mg of the powdered hydroxyapatite in 200 ml of acetate buffer under various conditions and containing different amounts of strontium or phosphate or both occurred at 30 C. The rate of dissolution was determined by procedures described before,[5,6] which involved calcium or phosphate analysis, or both, of solution aliquots removed from the reaction system as a function of time.

The amount of hydroxyapatite dissolved reached a constant level with time, usually after several hours. The concentrations of calcium and phosphate present in this plateau region were used to calculate the solubility product according to equation 19.

ANALYTICAL PROCEDURE.—Calcium concencentrations were determined by use of an

TABLE 1

EQUILIBRIUM CONSTANTS FOR THEORETICAL CALCULATIONS

	Thermodynamic Constants (moles/liter)	Corrected Constants*
K_{2p}	6.40×10^{-8}	1.92×10^{-7}
K_{3p}	4.73×10^{-13}	1.43×10^{-12}
K_{HA} (acetic)	1.75×10^{-5}	2.98×10^{-5}
K_w	1.00×10^{-14}	1.79×10^{-14}

Note: All diffusion coefficients were taken as 1×10^{-5} cm^2 second^{-1}.

* These corrections were based on activity coefficients established for ionic strength in the range of 0.1 to 0.2. The activity coefficients of calcium and strontium ions were assumed to be the same.

atomic absorption spectrophotometer.[d] The analytical procedures were essentially the same as described previously[5,6] at $\lambda = 211$ A. The analytical procedure for phosphate was based on the method of Dickman and Bray.[9] The acid-ammonium molybdate solution was prepared by adding 15 gm ammonium molybdate to 1,000 ml 3.5 *N* hydrochloric acid solution. This stock solution was made up fresh every two months. The remainder of the procedure was the same as that described previously.[5,6]

Results

DISSOLUTION RATES AND SOLUBILITIES.—Figure 3 shows typical raw dissolution data obtained with the hydroxyapatite crystals in various acetate buffer solutions. The amount of apatite dissolved is plotted against time. The initial data points are important because the experimental dissolution rates of apatite in all the solvents studied were obtained by taking the initial slopes of the dissolution curves such as those shown in Figure 3. The plateau regions of the dissolution curves represent apparent saturation of the solvents with apatite. Data in these regions are a direct measure of the apparent solubilities of apatite in the solvents.

The experimental dissolution rates, *Je*, and the apparent solubilities, C_s, for the TVA hydroxyapatite in acetate buffers containing various concentrations of phosphate, calcium, and strontium ions at three pH values are shown in Table 2. These are the key data used in the critical examination of the proposed physical model and in defining the role of strontium in apatite dissolution.

Figure 4 shows the effect of strontium and phosphate ions on the dissolution of apatite in acetate buffers at various pH values. The results are presented as the percent of the rate without strontium or phosphate ions vs the concentration of strontium ions present in the buffer.

The strontium and phosphate, individually, significantly inhibited the hydroxyapatite dissolution rate. The dissolution rates generally decreased with increasing concentrations of strontium ions, except at the lowest strontium level of 1×10^{-3} *M* where no effect on the dissolution rate was observed (pH, 4.0 and 4.5). Also, the absence of strontium-phosphate showed an inhibitory effect that increased with increased phosphate concentration and increasing pH. This agrees with our previous work.[5,6]

[d] Model 303, Perkin-Elmer Corporation, Norwalk, Conn.

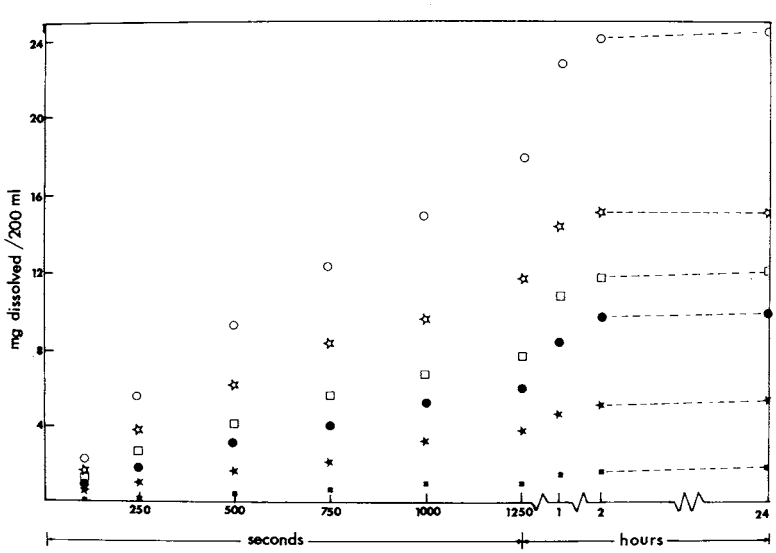

FIG 3.—Dissolution rate of hydroxyapatite in 0.5 *M* NaCl, 0.05 *M* acetate buffers (pH, 4.5) at various strontium and phosphate concentrations. ○ control (no strontium, no phosphate); ☆ 1×10^{-2} *M* Sr; □ 5×10^{-3} *M* phosphate; ● 1×10^{-3} *M* Sr, 5×10^{-3} *M* phosphate; ★ 3×10^{-3} *M* Sr, 5×10^{-3} *M* phosphate; ■ 1×10^{-2} *M* Sr, 5×10^{-3} *M* phosphate.

TABLE 2

DISSOLUTION RATES (*Je*) AND APPARENT SOLUBILITIES (*Cs*) OF TVA HYDROXYAPATITE (100 mg) IN ACETATE BUFFERS

0.05 *M* Acetate Buffers				
pH	$(PO_4^{\equiv})$ $\times 10^{-3}$ (molar)	(Sr^{2+}) $\times 10^{-3}$ (molar)	$Je \times 10^{-8}$ (moles/sec)	$Cs \times 10^{-6}$ (molar)
4.0	0.0	0.0	45.402	24.20
	0.0	3.0	33.132	22.00
	0.0	10.0	26.508	17.25
	3.0	0.0	44.802	20.65
	3.0	1.0	18.834	19.30
	3.0	3.0	14.454	14.25
	3.0	10.0	9.636	9.00
	30.0	0.0	10.884	10.75
	30.0	1.0	7.950	8.06
	30.0	3.0	5.190	5.05
4.5	0.0	0.0	16.488	12.30
	0.0	1.0	16.014	12.01
	0.0	3.0	11.538	9.05
	0.0	10.0	9.462	7.50
	1.0	0.0	9.540	7.48
	1.0	1.0	6.294	7.00
	1.0	3.0	4.671	3.55
	1.0	10.0	1.903	1.52
	3.0	0.0	7.482	7.04
	3.0	1.0	5.677	6.53
	3.0	3.0	3.128	3.37
	3.0	10.0	1.329	1.19
	5.0	0.0	6.900	6.00
	5.0	1.0	5.088	5.07
	5.0	3.0	2.740	2.74
	5.0	10.0	0.495	1.10
5.0	0.0	0.0	12.663	4.05
	0.0	1.0	6.604	3.25
	0.0	3.0	4.560	2.55
	1.0	0.0	6.307	6.30
	1.0	1.0	2.786	1.26
	1.0	3.0	1.650	0.38

When 3×10^{-3} *M* phosphate and 1×10^{-3} *M* strontium were present in acetate buffer at pH 4.0, the apatite dissolution rate decreased by 60%, although no inhibitory effect was detected when either was present alone at the same concentrations. Furthermore, this strontium-phosphate inhibition synergism at pH 4.0 was evident in all of the experiments at the higher strontium and phosphate concentrations. This strontium-phosphate interaction also was observed at other pH values. It is this synergism that supports the idea that the rate-determining step involves a complex, the composition of which includes strontium and phosphate.

CALCULATED RESULTS FROM DISSOLUTION RATE DATA.—Figure 5 shows the results of model calculations based on ten experimental dissolution rates for hydroxyapatite crystals in acetate buffers (pH, 4.5) containing phosphate and strontium ions. The activity product, K_{ap}, of the calcium-strontium apatite complex, $Ca_{10-n}Sr_n(PO_4)_6(OH)_2$, was calculated as a function of n, the number of strontium ions per formula of the complex. The results are presented as plots of log K_{ap} vs n ranging from 0 to 10. The K_{ap} calculations show the largest spreads at the low ($n = 0$) and high ($n = 10$) n values; the spread in log K_{ap} is at a minimum when n is about 4. Here, the log K_{ap} values range from about -131 to -135, which corresponds to a mean value of about -133 ± 2.

Similar results calculated from dissolution rate data obtained in seven buffer conditions at pH 4.0 are shown in Figure 6. K_{ap} of 10^{-133} obtained from a spread in log K_{ap} of -131 and -135 and n of 4 are shown. The minimum spread in log K_{ap} occurred at about $n = 4$, where the corresponding log K_{ap} was -133 ± 2. Figure 7 shows the results from four buffer conditions at pH 5.0. Values of log $K_{ap} = -130.5 \pm 0.5$ and $n = 4$ appear to be the best choice. These calculations show that results of hydroxyapatite dissolution under a total of 21 buffer conditions (shown in Figs 5 to 7) are consistent with equations 16 and 17 and the Table 2 data, when values of 4 and $10^{-130.5}$ to 10^{-133} are assigned to n and K_{ap}, respectively.

CALCULATED RESULTS FROM SOLUBILITY DATA.—Figure 8 gives the results calculated using the apparent solubility data in the buffers with a pH of 4.5. A minimum spread in log K_{ap} from -131 to -135 occurred at $n \simeq 4$. Figures 9 and 10 show similar results of -134 and -133.5 for log K_{ap} at $n = 4$ from solubility data obtained with buffered pH 4.0 and pH 5.0.

Discussion

A minimum spread in log K_{ap}, ranging from -131 to -135, has consistently appeared at $n \simeq 4$ (Figs 5-10). These results were deduced from the self-consistent treatment of the dissolution rate data with the model under 21 buffer conditions and from the treatment of the solubility data obtained from the same experiments. Based on

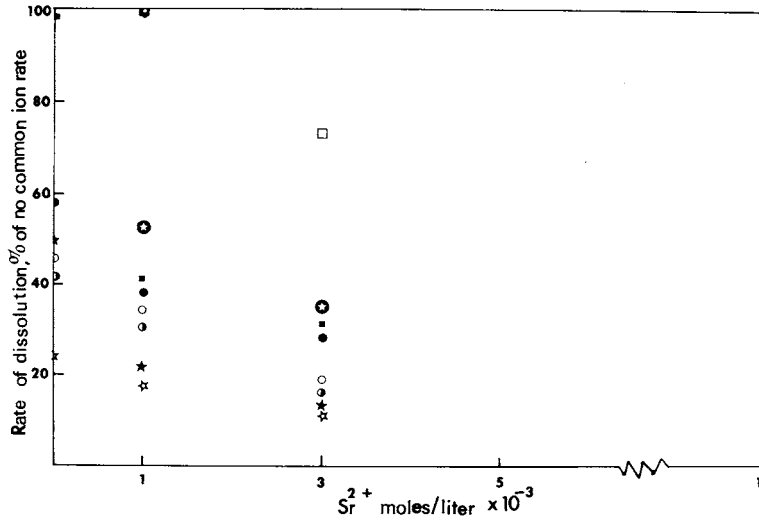

FIG 4.—Effect of strontium ions on initial dissolution rates of hydroxyapatite (TVA) in 0.5 *M* NaCl, 0.05 *M* acetate buffer at various pH and phosphate concentrations. pH 4.0: □ 0.0 *M* phosphate, ■ 3×10^{-3} *M* phosphate, ☆ 3×10^{-2} *M* phosphate; pH 4.5: ◒ 0.0 *M* phosphate, ● 1×10^{-3} *M* phosphate, ◑ 5×10^{-3} *M* phosphate; pH 5.0: ✪ 0.0 *M* phosphate, ★ 1×10^{-3} *M* phosphate.

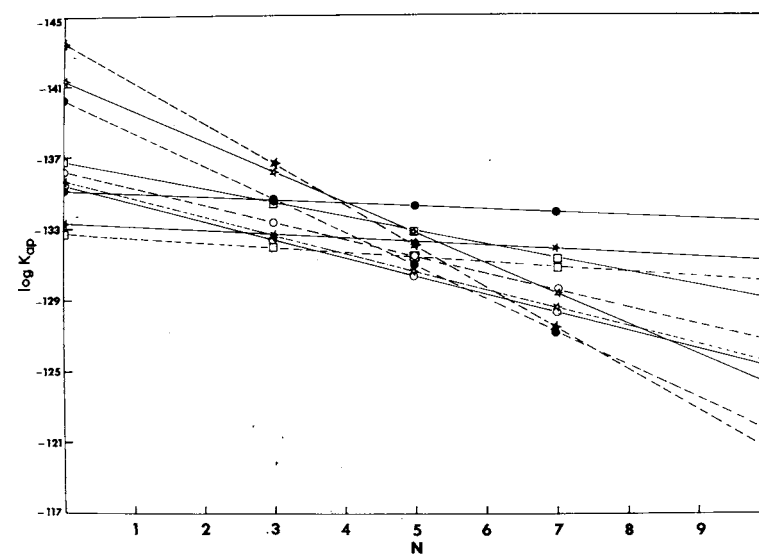

FIG 5.—Calculations of log K_{ap} as a function of n from initial dissolution rates of hydroxyapatite (TVA), 0.05 *M* acetate buffer (pH, 4.5) containing 0.5 *M* NaCl and various concentrations of strontium and phosphate.

—○—○— 1×10^{-2} *M* Sr;
—●—●— 1×10^{-3} *M* Sr, 1×10^{-3} *M* phosphate;
—□—□— 3×10^{-3} *M* Sr, 1×10^{-3} *M* phosphate;
—☆—☆— 1×10^{-2} *M* Sr, 1×10^{-3} *M* phosphate;
—★—★— 1×10^{-3} *M* Sr, 3×10^{-3} *M* phosphate;
-○----○- 3×10^{-3} *M* Sr, 3×10^{-3} *M* phosphate;
-●----●- 1×10^{-2} *M* Sr, 3×10^{-3} *M* phosphate;
-□----□- 1×10^{-3} *M* Sr, 5×10^{-3} *M* phosphate;
-☆----☆- 3×10^{-3} *M* Sr, 5×10^{-3} *M* phosphate;
-★----★- 1×10^{-2} *M* Sr, 5×10^{-3} *M* phosphate.

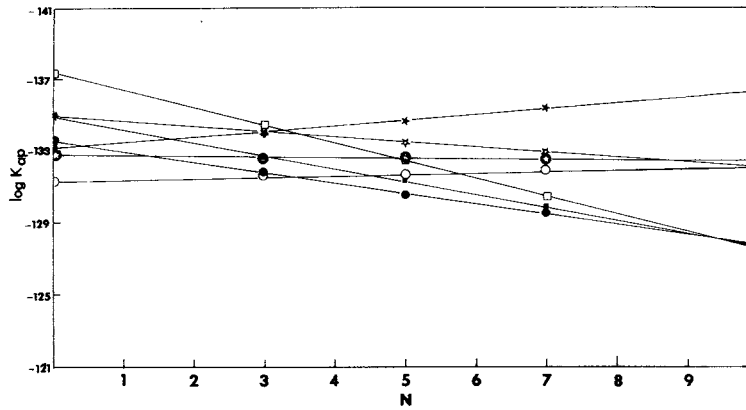

FIG 6.—Calculations of log K_{ap} as function of n from initial dissolution rates of hydroxyapatite (TVA), 0.05 M acetate buffer (pH, 4.0) containing 0.5 M NaCl and various concentrations of strontium and phosphate. ○ 3×10^{-3} M Sr; ● 1×10^{-2} M Sr; ★ 1×10^{-3} M Sr, 3×10^{-3} M phosphate; ☆ 3×10^{-3} M phosphate; □ 1×10^{-2} M Sr, 3×10^{-3} M phosphate; ◘ 1×10^{-3} M Sr, 3×10^{-2} M phosphate; ■ 3×10^{-3} M Sr, 3×10^{-2} M phosphate.

the large number of conditions involved, and the narrow spread in log K_{ap} at $n = 4$, it appears that the evidence supports the model shown in Figure 1 in which $n = 4$ and $K_{ap} = 10^{-133 \pm 2}$.

UNCERTAINTIES IN THE EXPERIMENTS AND IN THE CALCULATIONS WITH THE MODEL.—Even though the present analysis was done on the basis of a large number of experiments, it is difficult to provide a quantitative judgment on the reliability of the model with $K_{ap} = (Ca)^6 (Sr)^4 (PO_4)^6 (OH)^2 = 10^{-133}$. First, it is clear that for almost all of the data, when $n = 0$, 1, 2 or when $n = 8$, 9, or 10, the spread of the model calculated K_{ap} values are significantly beyond the expected experimental uncertainties. However, it may be argued that $n = 4$ is occasionally not better than $n = 3$ or $n = 5$ in some data sets that have been analyzed by the model.

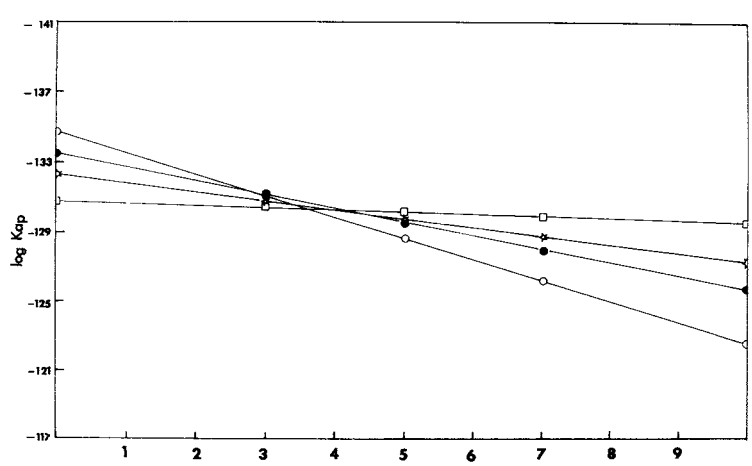

FIG 7.—Calculation of log K_{ap} as function of n from initial dissolution rates of hydroxyapatite (TVA), 0.05 M acetate buffer (pH, 5.0) containing 0.5 M NaCl and various concentrations of strontium and phosphate. ○ 1×10^{-3} M Sr; ● 3×10^{-3} M Sr; ☆ 1×10^{-3} M Sr, 1×10^{-3} M phosphate; □ 3×10^{-3} M Sr, 1×10^{-3} M phosphate.

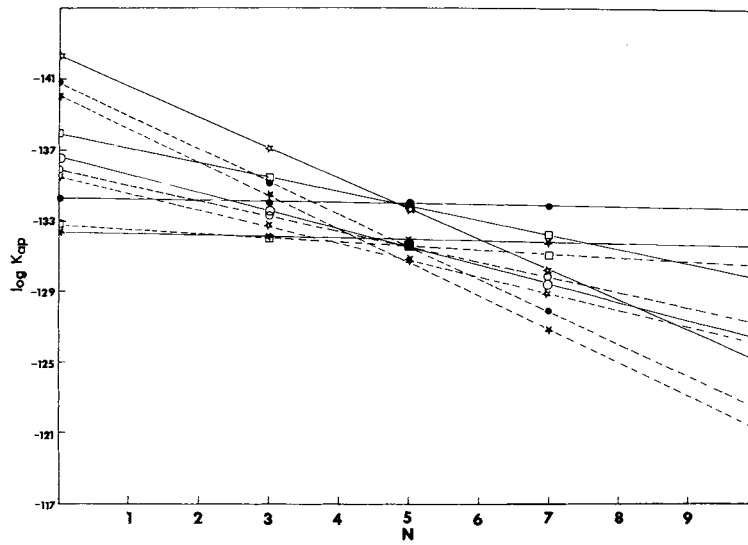

FIG 8.—Calculation of log K_{ap} as function of n from apparent solubilities of hydroxyapatite (TVA) in 0.05 M acetate buffers (pH, 4.5), 0.5 M NaCl containing various concentrations of strontium and phosphate.

—○—○— 1×10^{-2} M Sr;
—●—●— 1×10^{-3} M Sr, 1×10^{-3} M phosphate;
—□—□— 3×10^{-3} M Sr, 1×10^{-3} M phosphate;
—☆—☆— 1×10^{-2} M Sr, 1×10^{-3} M phosphate;
—★—★— 1×10^{-3} M Sr, 3×10^{-3} M phosphate;
-○----○- 3×10^{-3} M Sr, 3×10^{-3} M phosphate;
-●----●- 1×10^{-2} M Sr, 3×10^{-3} M phosphate;
-□----□- 1×10^{-3} M Sr, 5×10^{-3} M phosphate;
-☆----☆- 3×10^{-3} M Sr, 5×10^{-3} M phosphate;
-★----★- 1×10^{-2} M Sr, 5×10^{-3} M phosphate.

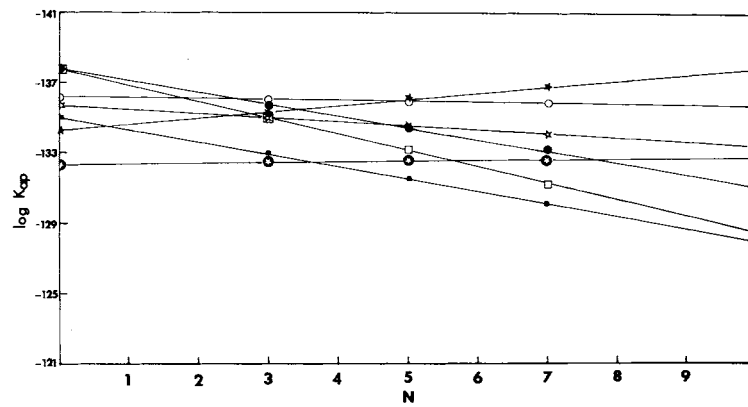

FIG 9.—Calculations of log K_{ap} as function of n from apparent solubilities of hydroxyapatite (TVA) in 0.05 M acetate buffers (pH, 4.0), 0.5 M NaCl containing various concentrations of strontium and phosphate. ○ 3×10^{-3} M Sr; ● 1×10^{-2} M Sr; ★ 1×10^{-3} M Sr, 3×10^{-3} M phosphate; ☆ 3×10^{-3} M Sr, 3×10^{-3} M phosphate; □ 1×10^{-2} M Sr, 3×10^{-3} M phosphate; ✪ 1×10^{-3} M Sr, 3×10^{-2} M phosphate; ■ 3×10^{-3} M Sr, 3×10^{-2} M phosphate.

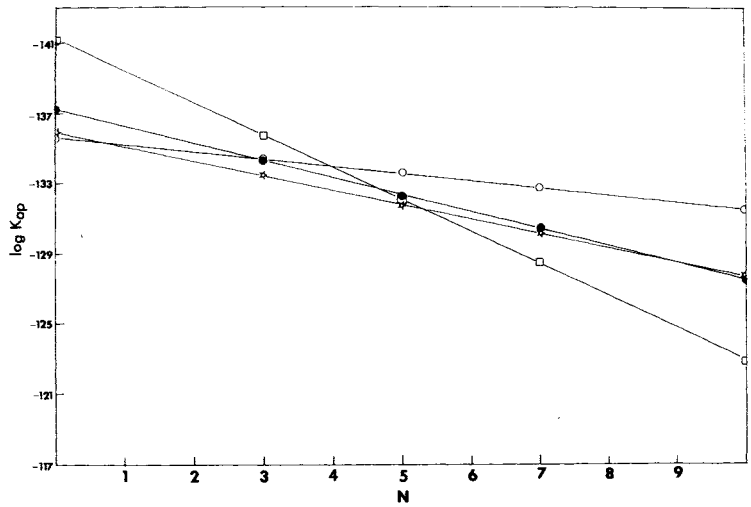

FIG 10.—Calculations of log K_{ap} as function of n from apparent solubilities of hydroxyapatite (TVA) in 0.05 M acetate buffers (pH, 5.0), 0.5 M NaCl containing various concentrations of strontium and phosphate. ○ 1×10^{-3} M Sr; ● 3×10^{-3} M Sr; ☆ 1×10^{-3} M Sr, 1×10^{-3} M phosphate; □ 3×10^{-3} M Sr, 1×10^{-3} M phosphate.

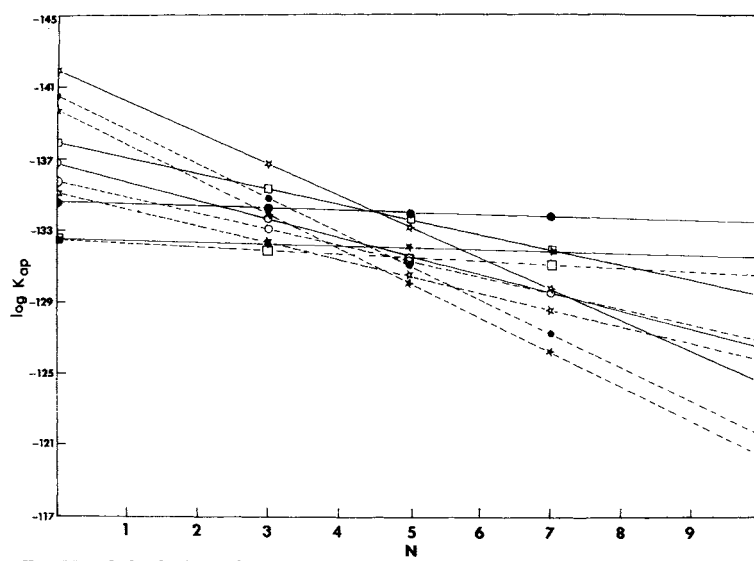

FIG 11.—Calculation of log K_{ap} as function of n after correcting for calcium and strontium complexes in apparent solubilities of hydroxyapatite (TVA) in 0.05 M acetate buffers (pH, 4.5), 0.5 M NaCl containing various concentrations of strontium and phosphate.

—○—○— 1×10^{-2} M Sr;
—●—●— 1×10^{-3} M Sr, 1×10^{-3} M phosphate;
—□—□— 3×10^{-3} M Sr, 1×10^{-3} M phosphate;
—☆—☆— 1×10^{-2} M Sr, 1×10^{-3} M phosphate;
—★—★— 1×10^{-3} M Sr, 3×10^{-3} M phosphate;
-○----○- 3×10^{-3} M Sr, 3×10^{-3} M phosphate;
-●----●- 1×10^{-2} M Sr, 3×10^{-3} M phosphate;
-□----□- 1×10^{-3} M Sr, 5×10^{-3} M phosphate;
-☆----☆- 3×10^{-3} M Sr, 5×10^{-3} M phosphate;
-★----★- 1×10^{-2} M Sr, 5×10^{-3} M phosphate.

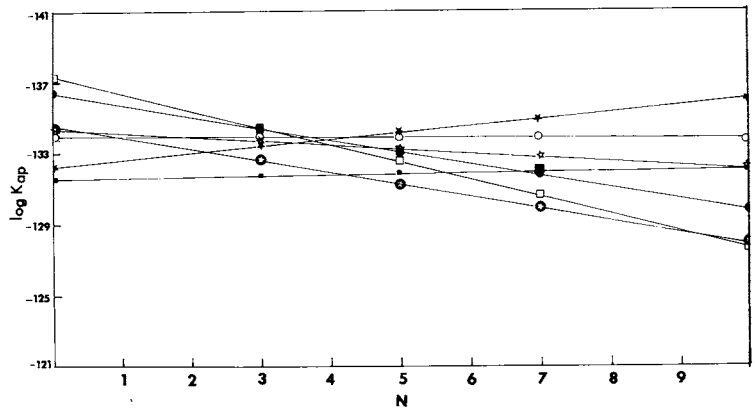

FIG 12.—Calculation of log K_{ap} as function of n after correction for calcium and strontium complexes in apparent solubilities of hydroxyapatite (TVA) in 0.05 M acetate buffers (pH, 4.0), 0.5 M NaCl containing various concentrations of strontium and phosphate. ○ 3×10^{-3} M Sr; ● 1×10^{-2} M Sr; ★ 1×10^{-3} M Sr, 3×10^{-3} M phosphate; ☆ 3×10^{-3} M Sr, 3×10^{-3} M phosphate; □ 1×10^{-2} M Sr, 3×10^{-3} M phosphate; ✪ 1×10^{-3} M Sr, 3×10^{-2} M phosphate; ■ 3×10^{-3} M Sr, 3×10^{-2} M phosphate.

Therefore, $n = 4$ should be offered as the tentative best n value.

A second important question is the reliability of the various basic mathematical relationships and the parameter values incorporated into the development of the model. With regard to this point, the neglect of the various complexes of calcium in the model might appear to be a serious limitation of equations 16 and 17. However, the complexes do not appear to be significantly important in the present situation. Figures 11 to 13 show K_{ap} calculations in which the CaB^+, CaHP, CaH_2P^+, SrB^+, SrHP, and

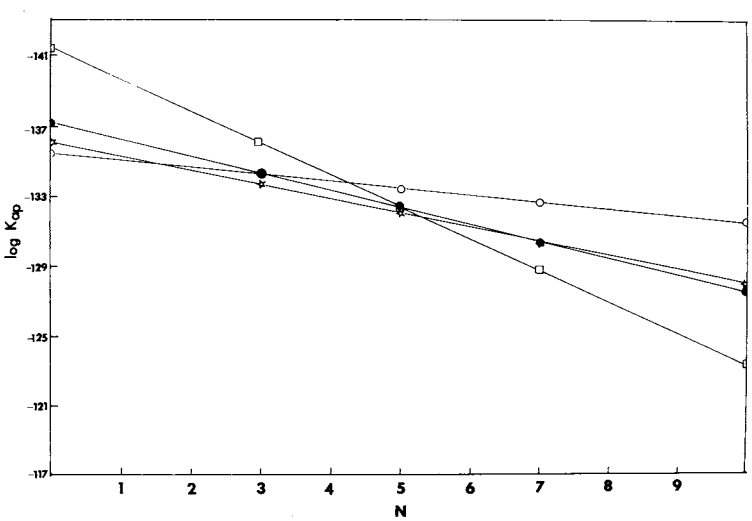

FIG 13.—Calculation of log K_{ap} as function of n after correction for calcium and strontium complexes in apparent solubilities of hydroxyapatite (TVA) in 0.05 M acetate buffers (pH, 5.0), 0.5 M NaCl containing various concentrations of strontium and phosphate. ○ 1×10^{-3} M Sr; ● 3×10^{-3} M Sr; ☆ 1×10^{-3} M Sr, 1×10^{-3} M phosphate; □ 3×10^{-3} M Sr, 1×10^{-3} M phosphate.

SrH_2P^+ complexes[e] were included in the K_{ap} calculations. These may be compared with the results in Figures 8 to 10. The consideration of the complexes in the calculations seems to make little difference to the main conclusions. The other errors and limitations in the model calculations, such as the neglect of electric diffusion potential and the uncertainties in the activity coefficients, should be rather small.

RELATIONSHIP OF THE PRESENT RESULTS TO OTHER WORK.—The substitution of surface intracrystalline calcium in apatite by strontium has been reported by many workers.[10-12] The finding that four of the ten calcium ions are substituted by strontium ions in forming the surface calcium-strontium apatite complex, $Ca_6Sr_4(PO_4)_6(OH)_2$, is specifically supported by the work of Neuman, Bjornerstedt, and Mulryan.[10] These investigators studied the incorporation of strontium onto synthetic hydroxyapatite crystals and showed that the substitution process is limited by the lattice sites of calcium. It was concluded that the six calcium ions in the screw-axis positions of the crystal lattice are less exchangeable and that the strontium ions are excluded. The calcium-strontium apatite complex that was derived from the present physical model treatment of dissolution kinetics data seems to be parallel to the results of Neuman, Bjornerstedt, and Mulryan[10] on equilibrium adsorption of strontium. This probably is not a coincidence.

The $Ca_6Sr_4(PO_4)_6(OH)_2$ complex probably would not be much more than the order of a unit-cell layer thick, since the dissolution rate experiments conducted in this study required no more than a couple of hours and the diffusion of strontium ions into the bulk crystal lattice is probably slow.

RELATIONSHIP TO PREVIOUS KINETICS STUDIES.—In earlier studies,[5,6,15] the physical model describing the solubility-diffusion-controlled dissolution kinetics of synthetic hydroxyapatite (TVA) was critically examined under conditions of common ions, low fluoride, buffer type, pH, and so on. A value of about 10^{-132} was calculated for the activity product of the apatite under a variety of conditions with the model. This value deduced from the dissolution rate data of apatite is much smaller than the thermodynamic value of 10^{-116} reported by Brown.[16] The possibility that poor choices for the model parameters might account for the difference between the "dynamic" activity product and the thermodynamic value has been discounted[17,18] as a result of careful work with model compounds that truly dissolve in acid buffers by a solubility-diffusion-controlled mechanism, for example, dicalcium phosphate dihydrate in acetate buffers. Therefore, it has been proposed[19] that TVA apatite dissolves in weak acid buffers by a false solubility-diffusion-controlled mechanism in which the reaction rates are effectively both "surface-controlled" and bulk-diffusion-controlled. The governing TVA hydroxyapatite activity product for the reaction might be equated to a false solubility product, the value for which is consistently about 10^{-131} to 10^{-133}.

The K_{ap} value for the proposed $Ca_6Sr_4(PO_4)_6(OH)_2$ complex is essentially identical to the parent entity $Ca_{10}(PO_4)_6(OH)_2$ and also the "fluorapatite" counterpart, $Ca_{10}(PO_4)_6F_2$, for which the dynamic K_{ap}[15] value was about 10^{-130} to 10^{-132}. Thus, it seems that such surface complexes may be a common occurrence for hydroxyapatite and can play important roles in governing the reaction kinetics in many situations. We anticipate that reaction rate-determining complexes of the type $Ca_{10-n}M_n(PO_4)_6(F)_2$ may govern rates of hydroxyapatite reaction when phosphate, fluoride, and a metal ion are present simultaneously in the reaction media. The clinical implication of this is that an inhibition synergism among phosphate, fluoride, and a foreign metal ion may exist and alter dental caries susceptibility.

Conclusions

A physical model was presented in an attempt to study critically the mechanistic role of strontium in inhibiting the dissolution rate of hydroxyapatite in acidic media. Experiments were conducted with synthetic hydroxyapaite (TVA). Initial dissolution rates and apparent solubilities of apatite were determined as a function of phosphate concentrations, strontium ion concentrations, and pH in acetate buffers.

[e] Thermodynamic equilibrium constant used are $CaB^+ = 18$, $SrB^+ = 15$[13], $CaH_2P^+ = 5.06$, $CaHP = 255.0$, $SrH_2P^+ = 5.06$, and $SrHP = 2.55$[14]. These values were corrected for the activity coefficient in the calculations.

Systematic and self-consistent treatment of the experimental data with the proposed model suggest that the inhibitory effect of strontium may be due to the formation of a calcium-strontium apatite complex of the composition $Ca_6Sr_4(PO_4)_6(OH)_2$ at the hydroxyapatite crystal surface. Furthermore, this complex may have the character of an "activated complex" that controls the dynamic conditions at the crystal-solvent interface and gives an apparent solubility product of $10^{-132\pm1}$.

This work has shown that the roles played by foreign ions in enamel dissolution can be delineated by means of analyses based on physically well-defined models. It should provide the basis for future investigations of the roles of other foreign ions. Also, it is anticipated that synergistic inhibition involving two or more foreign ions (for example, fluoride plus strontium) may be analyzed by these techniques.

References

1. Losee, F.L., and Bibby, B.G.: Caries Inhibition by Trace Elements Other Than Fluorine, *NY State Dent J* 36: 15-19, 1970.
2. Curzon, M.E.J.; Adkins, B.L.; Bibby, B.G.; and Losee, F.L.: Combined Effect of Trace Elements and Fluorine on Caries, *J Dent Res* 49: 526-528, 1970.
3. Losee, F.L., and Ludwig, T.G.: Trace Elements and Caries, *J Dent Res* 49: 1229-1235, 1970.
4. Buonocore, M.G., and Bibby, B.G.: The Effects of Various Ions on Enamel Solubilities, *J Dent Res* 24: 103-108, 1945.
5. Higuchi, W.I.; Gray, J.A.; Hefferren, J.J.; and Patel, P.R.: Mechanism of Enamel Dissolution in Acid Buffers, *J Dent Res* 44: 330-341, 1965.
6. Higuchi, W.I.; Mir, N.A.; Patel, P.R.; Becker, J.W.; and Hefferren, J.J.: Quantitation of Enamel Demineralization Mechanisms: III. A Critical Examination of Hydroxyapatite Model, *J Dent Res* 48: 396-409, 1969.
7. Liang, Z.: Kinetics and Mechanism of Fluoride Uptake by Hydroxyapatite, PhD thesis, appendix IV, University of Michigan, 1971.
8. Tennessee Valley Authority: *Report No: 678,* Alabama: Wilson Dam, Nov 6, 1956.
9. Dickman, S.R., and Bray, R.H.: Calorimetric Determination of Phosphate, *Ind Eng Chem* 12: 665-668, 1940.
10. Neuman, W.F.; Bjornerstedt, R.; and Mulryan, B.J.: Synthetic Hydroxyapatite Crystals. II. Aging and Strontium Incorporation, *Arch Biochem Biophys* 101: 215-224, 1963.
11. Likins, R.C.; McCann, H.G.; Posner, A.S.; and Scott, D.B.: Comparative Fixation of Calcium and Strontium by Synthetic Hydroxyapatite, *J Biol Chem* 235: 2152-2156, 1960.
12. Sakeb, F.Z., and DeBruyn, P.L.: Surface Properties of Alkaline Earth Apatite, *J Electroanal Chem* 37: 99-118, 1972.
13. Nancollas, A.N.: Thermodynamics of Ion Association. Part II. Alkaline-Earth Acetates and Formates, *J Phys Chem* 60: 744-749, 1956.
14. Sillen, L.G., and Martell, A.E.: Stability Constants of Metal Ion Complexes, Special Publication No. 25, London: The Chemical Society, Burlington House, 1964.
15. Mir, N.A.; Higuchi, W.I.; and Hefferren, J.J.: The Mechanism of Action of Solution Fluoride Upon the Demineralization Rate of Human Enamel, *Arch Oral Biol* 14: 901-920, 1969.
16. Brown, W.E.: Behavior of Slightly Soluble Calcium Phosphates as Revealed by Phase Equilibrium Calculations, *Soil Sci* 90: 51-58, 1960.
17. Hodes, B., and Higuchi, W.I.: Dissolution Rate Studies of $CaHPO_4 \cdot 2H_2O$ Employing the Rotating Disk Method, abstracted, IADR *Program and Abstracts of Papers,* No. 186, 1970.
18. Hodes, B.: Dissolution Rate Studies of Some Calcium Phosphates Using the Rotating Disk Method, PhD thesis, University of Michigan, 1971.
19. Hodes, B., and Higuchi, W.I.: Dissolution Rate Studies with Synthetic Hydroxyapatite, abstracted, IADR *Program and Abstracts of Papers* No. 473, 1972.